

Magnetic edge states in Aharonov-Bohm graphene quantum rings

R. Farghadan,^{1,*} A. Saffarzadeh,^{2,3} and E. Heidari Semiromi¹

¹*Department of Physics, University of Kashan, Kashan, Iran*

²*Department of Physics, Payame Noor University, P.O. Box 19395-3697 Tehran, Iran*

³*Department of Physics, Simon Fraser University, Burnaby, British Columbia, Canada V5A 1S6*

(Dated: November 5, 2018)

The effect of electron-electron interaction on the electronic structure of Aharonov-Bohm (AB) graphene quantum rings (GQRs) is explored theoretically using the single-band tight-binding Hamiltonian and the mean-field Hubbard model. The electronic states and magnetic properties of hexagonal, triangular and circular GQRs with different sizes and zigzag edge terminations are studied. The results show that, although the AB oscillations in the all types of nanoring are affected by the interaction, the spin splitting in the AB oscillations strongly depends on the geometry and the size of graphene nanorings. We found that the total spin of hexagonal and circular rings is zero and therefore, no spin splitting can be observed in the AB oscillations. However, the non-zero magnetization of the triangular rings breaks the degeneracy between spin-up and spin-down electrons, which produces spin-polarized AB oscillations.

PACS numbers: 73.21.-b, 73.22.pr, 75.75.-c

I. INTRODUCTION

In nanoscience and nanotechnology, quantum ring nanostructures with phase-coherence phenomena, such as persistent currents and the Aharonov-Bohm (AB) oscillations, are considered as good candidates for quantum interference devices due to their unique topology¹⁻³. The existence of persistent current, a direct consequence of the AB effect⁴ in normal electronic mesoscopic rings pierced by a magnetic flux, was observed both theoretically⁵ and experimentally⁶ by pointing out that the flux quantum $\phi_0 = hc/e$ determines the period of the current. Moreover, the AB effect in metal rings⁶ and the flux dependence of persistent current in mesoscopic rings with spin in the absence of $e-e$ interaction were predicted⁷. With development of fabrication techniques, true quantum limit of nanoscopic rings containing only a few electrons was obtained by Lorke and coworkers⁸⁻¹⁰.

On the other hand, carbon based nanostructures, such as nanoribbons, quantum dots or flakes, and graphene quantum rings (GQRs), have been the target of intense scrutiny in theory and experiment since the possibility of controlling their energy spectrum and hence electronic and novel magnetic properties. Specially, in recent years, ring-type nanostructures made of carbon-based materials like carbon nanotubes¹¹ and two-dimensional graphene with the large mean free path of carriers provide new challenges in studying the persistent current and the AB effect¹². Furthermore, signatures of the AB oscillations in a graphene ring structure for the first time observed experimentally in a two-terminal setup¹² by clear magnetoconductance oscillations with the expected period corresponding to one magnetic flux quantum ϕ_0 . In addition, several studies concerning the AB effect in graphene were published in theory¹³⁻¹⁸ and experiment¹⁹⁻²¹.

Recently, based on a noninteracting electron model, the period of magnetic flux in the AB effect in narrow GQRs with zigzag boundary conditions has been studied²². However, graphene nanoribbons^{23,24}, triangular²⁵ and hexagonal GQRs²⁶ with zigzag edges are magnetized due to the $e-e$ interaction. This implies that to study a quantum interference

device based on a graphene nanoring with zigzag edges, many body effects even in a mean-field approximation must be included in the theory.

In this paper, the single-band tight-binding (TB) approximation and the mean-field Hubbard model are combined to investigate the electronic structures, magnetic properties, and AB oscillations of hexagonal, triangular and circular narrow graphene rings with zigzag edges. We show that there are drastic modifications in the amplitude and the position of AB oscillations due to the $e-e$ interaction specially near the Fermi energy. We also study the size effects on the electronic levels and localized magnetic moments of nanorings for different geometries. Spin-polarized AB oscillations are observed in the triangular rings in spite of other ring shapes. We note that an interesting feature of these Hubbard rings is that, despite being a strongly correlated electron system, it is easy to introduce physical effects such as impurity, disorder, magnetic and electric fields and external leads in the theory, which are usually much harder to be included in other models.

The paper is organized as follows: In section II, we present the single band TB approximation in the presence of $e-e$ interaction by using the half-filled Hubbard model within the Hartree-Fock approximation. In Section III, the electronic spectra and magnetic properties of hexagonal, triangular and circular GQRs, and the effect of $e-e$ interaction in the AB oscillations will be illustrated. Finally, we summarize our results in section IV.

II. MODEL AND METHOD

We simulate the electronic structure of three different GQRs geometries [shown in Fig. 1] using the π -orbital tight-binding model and Hubbard repulsion treated in the mean-field approximation. This formalism, which includes the $e-e$ interaction in the location of atomic sites, induces localized magnetic moments on the zigzag-edge atoms. We use the Hubbard Hamiltonian with a pure AB flux ϕ . Due to the presence of a vector potential associated with a uniform magnetic

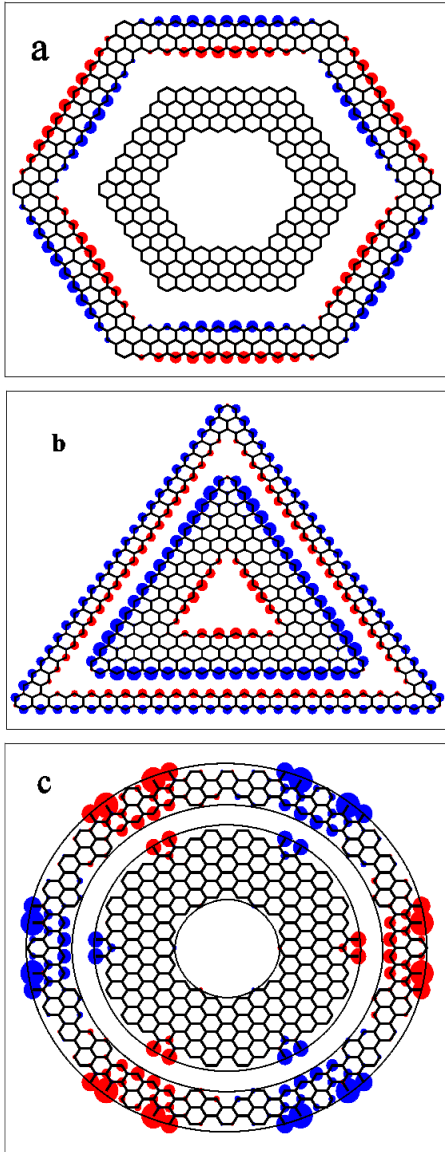


FIG. 1: (Color online) Schematic view of (a) hexagonal, (b) triangular, and (c) circular zigzag-edge graphene rings with distribution of the local magnetic moments. The blue (red) circles correspond to the majority (minority) spin electrons. The outer (narrow) hexagonal and triangular nanorings are described by W and L , where W is the number of benzene rings in the thickness of each ribbon and L is the number of one type of carbon atoms in the inner edge of each ribbon. In (a), $W = 2(3)$ and $L = 10(4)$ for the outer (inner) hexagonal ring, (b) $W = 3(1)$ and $L = 7(22)$ for the inner (outer) triangular ring, and (c) two circular rings with different width and size.

field, the hopping integrals between the nearest neighbors in the tight-binding Hamiltonian are modified by a phase factor²⁷ and as a result, the Hamiltonian for a ring with N lattice sites can be written as²³

$$H = \sum_{\langle i,j \rangle, \sigma} \left(t_{ij} c_{i,\sigma}^\dagger c_{j,\sigma} \right) + U \sum_{i,\sigma} \langle \hat{n}_{i,-\sigma} \rangle \langle \hat{n}_{i,\sigma} \rangle - \frac{1}{2} \langle \hat{n}_{i,\sigma} \rangle. \quad (1)$$

Here, the operator $c_{i\sigma}^\dagger$ ($c_{i\sigma}$) creates (annihilates) an electron with spin σ at site i and $n_{i\sigma} = c_{i\sigma}^\dagger c_{i\sigma}$ is a number operator. The first term in Eq. (1) describes the hopping of electrons between neighboring sites (kinetic term) where the hopping matrix element is defined as

$$t_{ij} = t \exp \left(\frac{ie}{\hbar c} \int_{\mathbf{r}_i}^{\mathbf{r}_j} \mathbf{A}(\mathbf{r}) \cdot d\mathbf{s} \right) \quad (2)$$

In this equation, \mathbf{r}_i is the position of carbon atom at site i , and \mathbf{A} is a vector potential in a symmetric gauge associated with the perpendicular magnetic field B which can be written as

$$\mathbf{A} = Br_0^2/2(-y/r^2, x/r^2, 0). \quad (3)$$

Indeed, the magnetic field B is applied only in the central region of absent atoms (antidot) for $r < r_0$ so that the magnetic flux ϕ is $\phi = B\pi(r_0^2)$ ²². The second term in Eq.(1) gives the repulsion between electrons occupying the same site. Accordingly, the magnetic moment at each site of carbon atoms can be expressed as

$$m_i = \langle S_i \rangle = (\langle \hat{n}_{i,\uparrow} \rangle - \langle \hat{n}_{i,\downarrow} \rangle)/2. \quad (4)$$

Note that, the on-site energy in the tight-binding Hamiltonian is set to zero, $t = -2.66$ eV is the transfer integral between all the nearest neighbor sites, and $U = 2.82$ eV is the Hubbard parameter which indicates the strength of on-site Coulomb interactions at each carbon sites of nanorings.

III. RESULTS AND DISCUSSION

In order to study the electronic states and magnetic properties of the nanorings, we start from anti-ferromagnetic configuration as an initial condition for each structure and solve the mean field Hubbard Hamiltonian self-consistently. As shown in Fig. 1, we consider three different types of zigzag-edges rings as hexagonal, triangular, and circular shapes. In the case of hexagonal and triangular rings [see Figs. 1(a) and 1(b)], we describe the number of benzene rings which forms the thickness of each ribbon by W and the number of carbon atoms in the inner edge of each ribbon by L . The hexagonal GQRs consist of six narrow nanoribbons and therefore have six-fold rotational symmetry, but the triangular rings with three nanoribbons have three-fold rotational symmetry. In addition, the circular graphene rings in the present form [see Fig. 1(c)] have six-fold rotational symmetry. The difference between the three quantum rings is that both the hexagonal and triangular rings have well-defined zigzag edges in both inner and outer edges, while the circular GQRs have both the zigzag and armchair edges.

In Fig. 1(a), the inner ring, i.e. the thicker structure with $W = 3$ and $L = 4$, consists of 288 carbon atoms, while the outer one, i.e. the thinner structure with $W = 2$ and $L = 10$, has 414 carbon atoms. The hexagonal graphene rings have the same number of A- and B-type atoms and each edge (inner or outer edge) consists of both types of atoms. Therefore, according to the Lieb's theorem²⁸, the total spin value

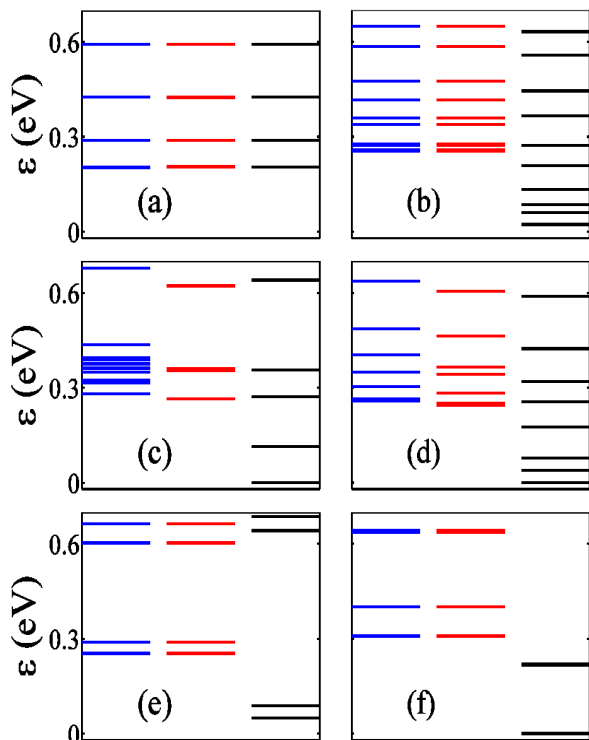


FIG. 2: (Color online) Energy levels near the Fermi level for three different types of zigzag-edges graphene rings. (a) ((b)) hexagonal ring with width $W=3(2)$, (c)((d)) triangular ring with width $W=3(1)$ and (e)((f)) thicker (thinner) circular ring. In the figures, the left and middle columns (blue and red lines) show energy spectrum for majority and minority spins, respectively, while the right column (black lines) shows energy level in the absence of electron-electron interaction.

is zero and each edge has an antiferromagnetic spin configuration. Furthermore, the magnetization of each zigzag edge in hexagonal rings strongly depends on the size and width of the ring. Specially for very small rings, the edge states on different sides of inner or outer ring boundaries are subject to strong hybridization, and therefore spontaneous spin polarization does not occur^{26,29}. In the case of thicker hexagonal ring which corresponds to the inner ring in Fig. 1(a), the spin polarization vanishes completely and a non-magnetic ground state is obtained. On the other hand, the total spin value for the thinner hexagonal ring is zero, similar to the thicker hexagonal graphene ring, while a nonzero spin with maximum value $S = 0.12$ is induced on the inner and outer edges. This means that, due to the $e - e$ interaction, an antiferromagnetic order forms in this type of nanorings²⁶ and the six-fold rotational symmetry is broken to three-fold symmetry [see the red and blue circles in Fig. 1(a)].

The two triangular graphene rings with different widths and sizes have been shown in Fig. 1(b). Both the inner ring (the thicker structure) with $W = 3$ and $L = 7$, and the outer one (the thinner structure) with $W = 1$ and $L = 22$ have the same 285 carbon atoms. However, the triangular graphene rings have different number of A- and B-type atoms and each edge

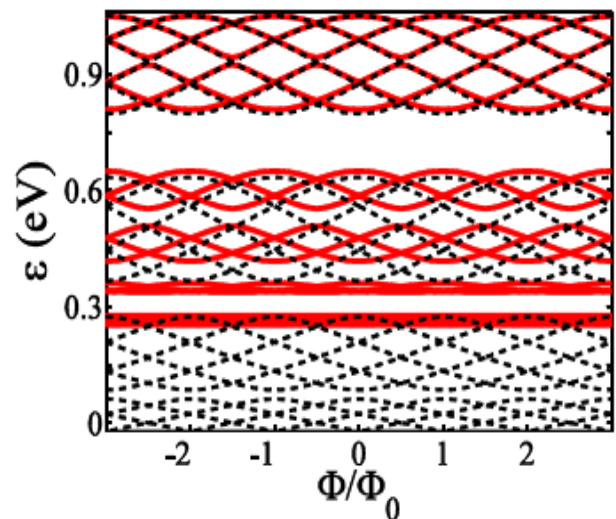


FIG. 3: (Color online) Aharonov-Bohm oscillations of the hexagonal graphene ring with $W = 2$ shown in Fig. 1(a). The solid (dashed) line shows the AB patterns with (without) considering the effect of $e - e$ interaction. The oscillations for spin-up and spin-down electrons are completely degenerate.

(inner or outer edge) has just one type of atoms. Therefore, in contrast to the hexagonal GQRs, the total spin value is non-zero and each edge has a ferromagnetic spin configuration and therefore, the $e - e$ interaction preserves the three-fold spatial symmetry. Furthermore, the triangular graphene rings have opposite spin configurations with different values of magnetic moments in both edges (inner and outer edges)²⁵. The total spin of the thicker (thinner) structure reaches $S = 4.5$ (1.5), which has a maximum value $S = 0.13$ (0.10) in the middle of zigzag edge segment, shown in Fig. 1(b).

The two symmetric circular graphene rings with six-fold rotational symmetry and different sizes has been shown in Fig. 1(c). Both circular rings have 330 atoms. In this type of rings, both zigzag and armchair edge states exist simultaneously in edge termination. However, the localized magnetic moments at the armchair edges almost vanishes. As a result, the magnetization of zigzag edge in circular GQRs strongly depends on the ring size and width, similar to the case of hexagonal nanorings. For example, a non-magnetic phase could be found for a circular ring with width 6 nm and 210 atoms. Although a nonzero magnetization with maximum spin value $S = 0.18$ is produced on the zigzag edges and also in the dangling bonds, the total spin of our circular rings is zero, due to the special symmetry between two different sub-lattices. The circular GQRs have opposite spin configurations in both edges and the magnetic moment in the inner edges is smaller than the outer edges, as shown by red and blue circles in Fig. 1(c).

In Fig. 2 we show how the single particle energy of the various rings with different sizes varies under the $e - e$ interaction. In order to compare the interacting and non-interacting systems, the energy spectra for electrons in both the systems are plotted near the Fermi energy that is set to zero. The energy levels for spin-up and spin-down electrons are also plot-

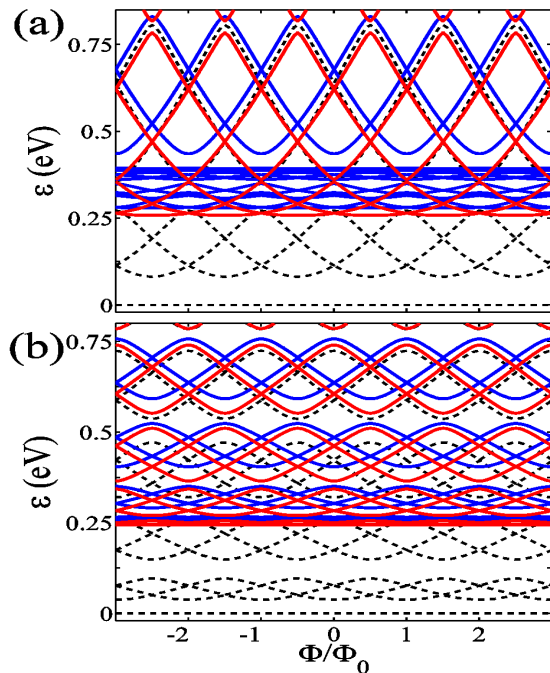


FIG. 4: (Color online) AB oscillations as a function of magnetic flux Φ for the triangular graphene rings with (a) $W = 3$ and (b) $W = 1$ (see Fig. 1(b)). The blue (red) solid lines show AB pattern for the majority (minority) spin electrons. The dashed lines show the AB patterns without $e - e$ interaction. Note that the oscillations for the majority and minority spin electrons are completely non-degenerate.

ted for comparison. In the case of hexagonal ring with width $W = 3$ (288 atoms), the interacting and non-interacting electrons have the same energy spectra as shown in Fig. 2(a). However, by increasing the length of hexagonal ring the effect of $e - e$ interaction increases and different energy levels, as shown in Fig. 2(b), are produced. Note that the energy spectra for spin-up and spin-down electrons are completely degenerate. In all cases, except the thicker hexagonal GQR, the $e - e$ interaction causes a significant change in the distribution of energy levels and induces gap at the Fermi energy. Although the energy spectrum changes by changing the size of the rings, the influence of $e - e$ interaction induces different energy spectra only in the majority and minority spin electrons of the triangular rings, as shown in Figs. 2(c) and 2(d). By comparing Figs. 2(a) and 2(b) and Figs. 2(e) and 2(f), one can see that the effect of interaction on the electronic levels of circular rings is much similar to the energy levels of hexagonal ones, and no spin splitting in the electronic levels of these types of nanorings can be expected.

Now, we examine the effect of $e - e$ interaction on the energy spectra in the presence of uniform magnetic flux threading the GQRs for various geometries. This interaction does not affect the energy spectra of the thicker hexagonal ring, i.e., $W = 3$ and $L = 4$, as we expect from Fig. 2(a). However, the evolution of AB oscillations induced by magnetic flux in the thinner hexagonal ring can be seen in Fig. 3. It is clear that, the period of such oscillations remains constant,

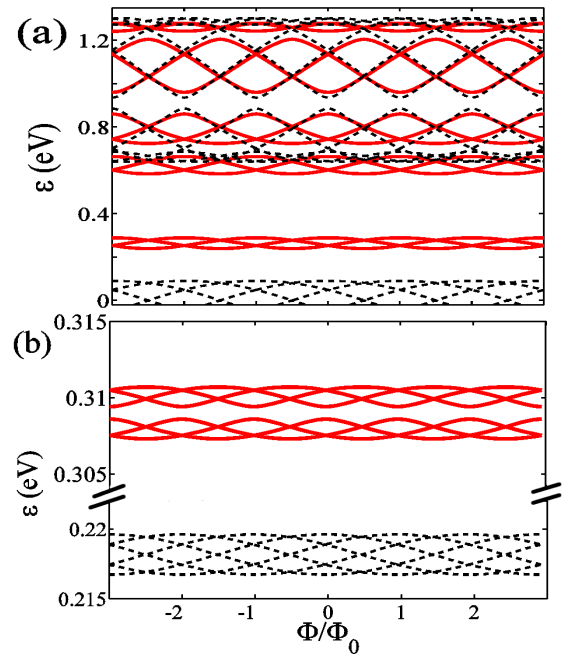


FIG. 5: (Color online) AB oscillations as a function of magnetic flux Φ for the circular graphene rings shown in Fig. 1(c). The solid (dashed) lines show AB pattern in the presence (absence) of $e - e$ interactions for (a) the thicker and (b) the thinner circular rings. The oscillations for spin-up and spin-down electrons are completely degenerate.

but the energy spectrum and the amplitude of the oscillations near the Fermi energy are strongly affected by the interaction. Due to the oscillations, the energy-gap value between energy levels is flux dependent and the amplitudes at the lowest energies (around 0.3 eV) are very short, which means that these states are less efficient in trapping magnetic flux. In addition, the six-fold rotational symmetry in the case of non-interacting electrons is broken to a three-fold rotational symmetry. These changes in the AB oscillations gradually disappear at higher energies where the change in the energy gaps decreases and eventually the AB patterns in the case of interacting and non-interacting electrons become similar. Note that the AB oscillations for the majority and minority spin electrons are completely degenerate. Moreover, our calculations showed that, by increasing the strength of $e - e$ interaction, the change in the energy gaps at the higher energy levels could also occur and the amplitude of AB oscillation slightly reduces.

The three energy distributions associated with the triangular rings as a function of magnetic flux in the case of interacting and non-interacting electrons have been illustrated in Fig. 4. For such nanorings, the AB patterns are somewhat complicated and the AB oscillations of majority and minority spin electrons near the Fermi energy are fully non-degenerate. A non-zero magnetization, which comes from magnetic moments, localized on the edge atoms, causes these spin-polarized oscillations in such triangular rings. The $e - e$ interaction induces a few energy levels along with very weak

oscillations for both majority and minority spin electrons. The thinner triangular ring, in the case of interacting and non-interacting electrons, shows similar behavior at higher energies and becomes nearly degenerate [see Fig. 4(b)]. With increasing the width of the ring, however, the net magnetization increases and the majority and minority spins show different behavior even at high energy levels [see Fig. 4(a)].

The AB oscillations for the two types of circular nanorings have been shown in Fig. 5. The main differences between the rings with interacting and non-interacting electrons fall within an energy window near the Fermi level. The $e - e$ interaction shifts the low-lying energy levels to higher energies and slightly decreases the amplitude of oscillations. In Fig. 5(a), the energy gap between AB oscillations increases at integer and half-integer values of ϕ , depending on the energy eigenvalues. Moreover, in the case of thinner ring, the amplitude of oscillations, which have been plotted in a small range of energies, is considerably weaker than that of the thicker one [see Fig. 5(b)].

The obtained results indicate that the $e - e$ interaction, which induces localized magnetic moments on the edges of GQRs, is able to reduce the magnetic symmetries compared to the structural symmetries and affects the AB oscillations dramatically, relative to the nanorings with non-interacting electrons. Note that this interaction cannot induce localized magnetic moments in the armchair nanorings and therefore, the AB oscillations are not affected by this kind of interaction.

IV. CONCLUSION

In summary, the influence of $e - e$ interaction on the AB pattern in zigzag-edge GQRs was studied by means of single-

band tight-binding Hamiltonian and the mean-field Hubbard model. This interaction induces localized magnetic moments on the the inner and outer edges of graphene nanorings which are strongly size and shape dependent. In addition, the interaction modifies the AB oscillations by changing energy levels near the Fermi energy and hence, a reduction in the amplitude of oscillations can be seen in all nanoring structures. The change in the amplitude and the position of AB oscillations is different from one nanoring to the other.

In the case of hexagonal and circular rings, the six-fold rotational symmetry changes to the three-fold symmetry due to the distribution of localized magnetic moments, while the degeneracy between the spin-up and spin-down electrons is not broken which causes unpolarized AB oscillations. On the other hand, due to the non-zero magnetic moment in the triangular rings, the degeneracy between the majority and minority of electrons is broken; therefore, spin-polarized AB oscillations can be expected in this type of nanorings. This polarization could provide us a possibility to generate the persistent spin current (SC) intrinsically in the zigzag-edge nanorings which are obtained by cutting and patterning the graphene sheets into the nanorings with special sizes and geometries. Thus, as well as being of fundamental interest, systematic experimental studies of magnetic edge states in zero-dimensional carbon structures like graphene nanorings might be useful for future spintronic applications.

ACKNOWLEDGMENTS

This work financially supported by university of Kashan under the Grant No. 228762.

* Electronic address: rfarghadan@kashanu.ac.ir

¹ A. D. Güçlü, P. Potasz, O. Voznyy, M. Korkusinski, and P. Hawrylak, Phys. Rev. Lett. **103**, 246805 (2009).

² V. Kotimäki and E. Räsänen, Phys. Rev. B **81**, 245316 (2010).

³ N. A. J. M. Kleemans, I. M. A. Bominaar-Silkens, V. M. Fomin, V. N. Gladilin, D. Granados, A. G. Taboada, J. M. Garcia, P. Offermans, U. Zeitler, P. C. M. Christianen, J. C. Maan, J. T. Devreese, and P. M. Koenraad, Phys. Rev. Lett. **99**, 146808 (2007).

⁴ Y. Aharonov, and D. Bohm, Phys. Rev. **115**, 485 (1959); **123**, 1511 (1961).

⁵ M. Büttiker, Y. Imry, and R. Landauer. Phys. Lett. A **96**, 365 (1983).

⁶ R. A. Webb, S. Washburn, C. P. Umbach, and R. B. Laibowitz, Phys. Rev. Lett. **54**, 2696 (1985).

⁷ D. Loss and P. Goldbart, Phys. Rev. B **43**, 13762 (1991).

⁸ J. M. Garcia, G. Medeiros-Ribeiro, K. Schmidt, T. Ngo, J. L. Feng, and A. Lorke, Appl. Phys. Lett. **71**, 2014 (1997).

⁹ A. Lorke, R. J. Luyken, Physica B **256**, 424 (1998).

¹⁰ A. Lorke, R. J. Luyken, A. O. Govorov, J. P. Kotthaus, J. M. Garcia, and P. M. Petroff, Phys. Rev. Lett. **84**, 2223 (2000).

¹¹ A. Bachtold, C. Strunk, J.-P. Salvetat, J.-M. Bonard, L. Forro, T. Nussbaumer, and C. Schönenberger, Nature, **397**, 673, (1999).

¹² S. Russo, J. B. Oostinga, D. Wehenkel, H. B. Heersche, S. S. Sobhani, L. M. K. Vandersypen, and A. F. Morpurgo, Phys. Rev. B **77**, 085413 (2008).

¹³ R. Jackiw, A. I. Milstein, S. Y. Pi, and I. S. Terekhov, Phys. Rev. B **80**, 033413, (2009).

¹⁴ P. Recher, B. Trauzettel, A. Rycerz, Y. M. Blanter, C. W. J. Beenakker, and A. F. Morpurgo, Phys. Rev. B **76**, 235404 (2007).

¹⁵ L. J. P. Xavier, J. M. Pereira, Andrey Chaves, G. A. Farias, and F. M. Peeters, Appl. Phys. Lett. **96**, 212 108 (2010).

¹⁶ J. Schelter, D. Bohr, and B. Trauzettel, Phys. Rev. B **81**, 195441 (2010).

¹⁷ D. S. L. Abergel, V. M. Apalkov, and T. Chakraborty, arXiv:0806.2854v1.

¹⁸ M. Zarenia, J. M. Pereira, A. Chaves, F. M. Peeters, and G. A. Farias, Phys. Rev. B **81**, 045431 (2010).

¹⁹ M. Huefner, F. Molitor, A. Jacobsen, A. Pioda, C. Stampfer, K. Ensslin, and T. Ihn, New Journal of Physics **12**, 043054 (2010).

²⁰ J. S. Yoo, Y. W. Park, V. Skakalova, and S. Roth, Appl. Phys. Lett. **96**, 143112 (2010).

²¹ D. Smirnov, H. Schmidt, and R. J. Haug, arXiv:1204.6281v2.

²² I. Romanovsky, C. Yannouleas, and U. Landman, Phys. Rev. B **85**, 165434 (2012).

- ²³ M. Fujita, K. Wakabayashi, K. Nakada, and K. Kusakabe, *J. Phys. Soc. Jap.* **65**, 1920 (1996).
- ²⁴ A. Saffarzadeh and R. Farghadan, *Appl. Phys. Lett.* **98**, 023106 (2011).
- ²⁵ P. Potasz, A. D. Güçlü , O. Voznyy, J. A. Folk, and P. Hawrylak, *Phys. Rev. B* **83**, 174441 (2011).
- ²⁶ M. Grujic, M. Tadic and F. M. Peeters, *Phys. Rev. B* **87**, 085434 (2013).
- ²⁷ R. E. Peierls, *Z. Phys. B: Condens. Matt.* **80**, 763 (1933).
- ²⁸ E. H. Lieb, *Phys. Rev. Lett.* **62**, 1201 (1989).
- ²⁹ J. Fernandez-Rossier and J. J. Palacios, *Phys. Rev. Lett.* **99**, 177204 (2007).